GPS-BASED NAVIGATION AND ORBIT DETERMINATION FOR THE AMSAT AO-40 SATELLITE

George Davis
Emergent Space Technologies, LLC

Michael Moreau, Russell Carpenter, Frank Bauer
NASA Goddard Space Flight Center

Abstract

The AMSAT OSCAR-40 (AO-40) spacecraft occupies a highly elliptical orbit (HEO) to support amateur radio experiments. An interesting aspect of the mission is the attempted use of GPS for navigation and attitude determination in HEO. Previous experiences with GPS tracking in such orbits have demonstrated the ability to acquire GPS signals, but very little data were produced for navigation and orbit determination studies. The AO-40 spacecraft, flying two Trimble Advanced Navigation Sensor (TANS) Vector GPS receivers for signal reception at apogee and at perigee, is the first to demonstrate autonomous tracking of GPS signals from within a HEO with no interaction from ground controllers. Moreover, over 11 weeks of total operations as of June 2002, the receiver has returned a continuous stream of code phase, Doppler, and carrier phase measurements useful for studying GPS signal characteristics and performing post-processed orbit determination studies in HEO. This paper presents the initial efforts to generate AO-40 navigation solutions from pseudorange data reconstructed from the TANS Vector code phase, as well as to generate a precise orbit solution for the AO-40 spacecraft using a batch filter.

1. Introduction

The flight of a GPS receiver on the AO-40 spacecraft was conceived in the mid-1990s as a low cost experiment utilizing existing receiver technology to demonstrate the feasibility of tracking GPS signals in a HEO. Some of the original goals for the AO-40 GPS experiment included demonstrating the operation of a GPS receiver in a HEO with no interaction from ground controllers; returning signal level measurements to map the GPS satellite antenna patterns above the constellation; and generating orbit and attitude solutions for the AO-40 spacecraft for operational use.

The first high altitude GPS experiments took place before the AO-40 spacecraft was launched. In late 1997, the TEAMSAT/YES[1] and EQUATOR-S[2] spacecraft became the first known examples of GPS signals being tracked above the GPS constellation using existing low Earth orbit (LEO)-heritage GPS receivers. Limitations in the receiver acquisition functions at high altitudes were overcome by manually commanding the receiver to track specific GPS satellites. The US Air Force Academy-sponsored Falcon Gold satellite took a different approach, using a "sampling receiver" to record sparse samples of the GPS spectrum from a geostationary transfer orbit[3]. The normal receiver processing functions were then performed on the ground in post-processing. At the time, these experiments were assumed to be the first ever examples of GPS tracking in a HEO, or from above the GPS constellation. Then in September 2000 the first public disclosure was made of a restricted US Department of Defense satellite program that had developed a successful GPS-based orbit determination system for a geostationary satellite[4]. Similar to Falcon Gold, this program used a distributed GPS receiver architecture consisting of an analog translator on the spacecraft and a ground-based receiver and processing system. These early experiments achieved some important milestones, including GPS signals tracked to altitudes higher than 60,000 km, successful tracking of GPS side lobe signals, and a GPS-based orbit determination system for a geostationary satellite.

The GPS experiment on the AO-40 spacecraft was first activated for approximately six weeks starting in September, 2001, and was reactivated on May 11, 2002. Initial results from the GPS receiver were presented in February, 2002[5]. The apogee GPS receiver on AO-40 has demonstrated the ability to operate autonomously and track GPS signals anywhere within its HEO, despite inherent limitations in the receiver due to the fact it was not designed to operate above the GPS constellation. It has successfully tracked weak GPS signals near apogee, as well as signals with extremely high Doppler shifts around perigee. Peak signal levels measured when the spacecraft was near its approximate 60,000 km altitude apogee were about 48 dB-Hz. This performance has been achieved while the spacecraft is spin-stabilized, which effectively reduces the field of view of the GPS antennas and introduces amplitude variations in the received signal levels. While capable of performing real time position and attitude solutions, none have been returned.

One of the significant milestones achieved in this experiment was the autonomous acquisition and tracking of GPS signals throughout the orbit without intervention from the ground. Another achievement is simply the amount of data that has been successfully returned, providing important information about GPS signal characteristics measured above the GPS constellation, and a resource for the study of GPS-based orbit determination in a HEO. This paper presents the early efforts to generate AO-40 navigation solutions from pseudorange data reconstructed from the TANS Vector code phase, as well as to generate a precise orbit solution for the AO-40 spacecraft from the GPS data.

2. The AO-40 Spacecraft and GPS Experiment

The AO-40 satellite is the latest in a series of low-cost spacecraft built by the Radio Amateur Satellite Corporation, or AMSAT, designed for radio amateurs to experience satellite tracking and to participate in radio propagation experiments. The spacecraft was launched into a geostationary transfer orbit on November 16, 2000 from Kourou, French Guiana, and was ultimately placed into the HEO depicted in Figure 1, with nominal elements given in Table 1. The AO-40 satellite is currently in a spin-stabilized attitude with the spin axis indicated in Fig. 1 (the GPS antennas are aligned with the spin axis, pointing towards nadir at apogee and towards zenith at perigee). Amateur radio operators have access to the spacecraft during the high altitude portions of each orbit, when the communications antenna arrays (indicated by the arrow) are directed towards nadir.

The AO-40 spacecraft carries two TANS Vector GPS receivers. The TANS Vector is a 6-channel, L_1, C/A-code GPS receiver[6], which has been used for real time orbit and attitude determination applications in LEO. Each receiver has one master antenna and three slave antennas multiplexed off the six receiver channels to measure differential carrier phase for determining host platform attitude. Code phase and Doppler from the master antenna are used for host platform position and velocity determination. In order to compensate for the increased path lengths and reduced GPS signal levels expected at high altitudes, Receiver 1 uses an additional pre-amplifier stage and high gain antennas. A photograph of the AO-40 spacecraft showing the four high gain GPS antennas as well as the other communications antennas is provided in Fig. 2. This side of the spacecraft is oriented in the direction of the arrow in Fig. 1. Receiver 2 is connected to four hemispherical patch antennas, mounted on the opposite side of the spacecraft.

In the current spin stabilized attitude, the high gain GPS antennas connected to Receiver 1 are favorably aligned both at apogee (nadir) and perigee (zenith). Because this provides good GPS coverage throughout the orbit, only Receiver 1 has been operated to date. The antennas are aligned with the nominal spin axis, so although the vehicle is spinning, the fields of view of the antennas are essentially constant.

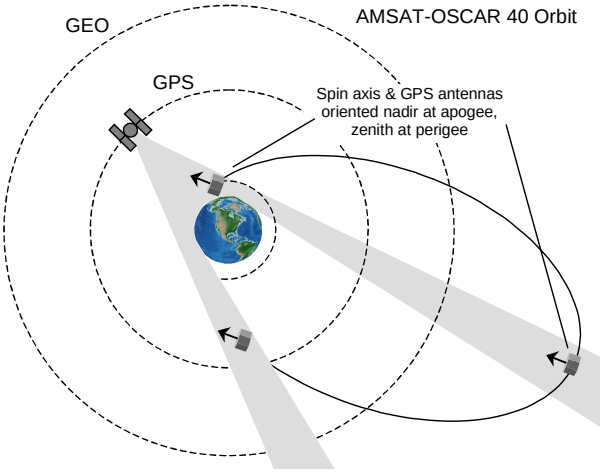

Figure 1. AO-40 Orbit and Attitude

Table 1. Nominal Orbit Parameters for AO-40

Orbit Parameter	Value
Semimajor Axis (km)	36,245
Perigee Height (km)	1,042
Apogee Height (km)	58,691
Eccentricity	0.797
Inclination (deg)	6.04
Period (hours)	19.1

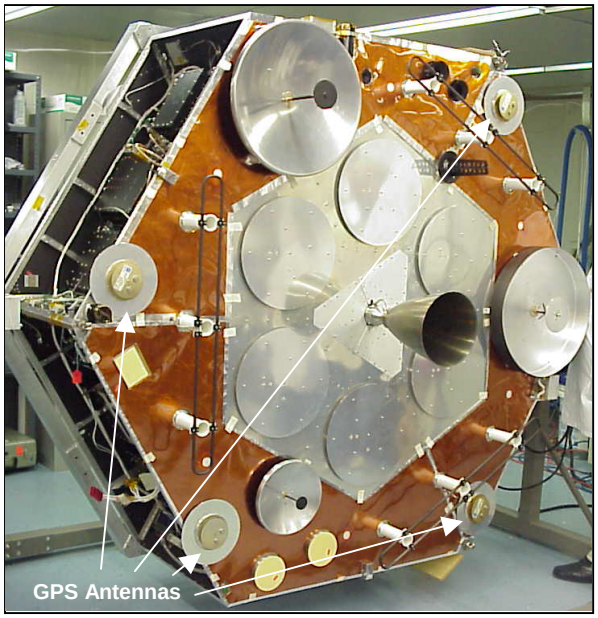

Figure 2. AO-40 Spacecraft

The normal satellite selection logic in the TANS Vector assumes that the receiving antennas are always oriented towards zenith, so a minor yet important software modification was made to disable this logic and force the receiver to use a "random search" acquisition process. This is one example of an aspect of the receiver design that was based on the assumption it would always be operated on or near the surface of the Earth. The "random search" acquisition mode creates the possibility that some visible GPS satellites may be missed, particularly when the dynamics are highest around perigee; however, it allows the receiver to perform the basic acquisition process autonomously, without any help from ground controllers. Without this change, it would have been impossible for this receiver to track satellites when above the GPS constellation.

The digital communications processor on AO-40 provides digital store and forward capabilities for users of the spacecraft, and serves as the communications path for interacting with the GPS receiver (and other) experiments. The binary data streams from the GPS receivers are binned into one-hour files which are downloaded to a suitably equipped ground station. Additional ground processing steps are performed to extract individual packets of data reported by the receiver. The TANS Vector reports the following GPS observables: code phase, carrier phase, Doppler, and signal to noise ratio (SNR) measured through the master antenna, and differential phase and SNR measured through each of the three slave antennas. The receiver is capable of returning real-time position, velocity, clock, and attitude solutions when four or more satellites are tracked simultaneously.

3. TANS Vector Pseudorange Recovery Algorithm

The code phase measurement from the TANS Vector is related to the pseudorange used to compute traditional GPS navigation or point solutions whenever 4 or more GPS space vehicles (SVs) are being tracked. For real-time navigation and post-processed orbit determination, it is the pseudorange, ρ, not the code phase, which is desired. It is formed in a GPS receiver by measuring the transit time of the GPS carrier signal multiplied by the speed of light:

$$\rho = c\left(t_{gps} - t_r\right) = c\left\{t_{gps_{true}} + \Delta t_{gps} - \left(t_{r_{true}} + \Delta t_r\right)\right\} \quad (1)$$

where t_{gps} is the time of transmission from the GPS satellite, and t_r is the time of reception. Both are modeled as the true time plus a timing bias. These biases, as well as atmospheric propagation delays, cause the pseudorange to deviate from the true range.

The Coarse/Acquisition (C/A)-code has a length of 1023 chips and a chipping rate of 1.023 MHz. As a result, the C/A-code repeats every millisecond (ms), and the code length corresponds to approximately 300 km of range. The pseudorange can thus be separated into two components: the integer number of 300 km C/A-code epochs, Δ, measured between signal transmission by the GPS satellite and reception by the GPS receiver, plus a fractional part, f, which is the code phase. This relationship is written as:

$$\rho = n\Delta + f \quad (2)$$

The objective in reconstructing the TANS Vector pseudorange from the code phase is thus to determine n, the number of integer C/A-code repeats. To do so, the line-of-sight range between the receiver and the transmitter must be known, as well as the receiver and GPS satellite clock biases. If the receiver is computing navigation solutions, as it would if it were in LEO, then its position and clock biases are known. The GPS satellite positions and clock biases are known from the broadcast ephemeris. The generalized algorithm for recovering pseudorange from the TANS Vector code phase is as follows:

- Get the receiver position, $\vec{x}_r$, and clock bias, Δt_r, from the point solutions
- Get the GPS satellite positions, $\vec{x}_{gps}$, and clock biases, Δt_{gps}, from the broadcast ephemeris
- Compute the modeled pseudorange:

$$\rho_{\text{mod}} = \left\|\vec{x}_{gps} - \vec{x}_r\right\| + c\left(\Delta t_{gps} - \Delta t_r\right) \quad (3)$$

- Compute the C/A-code repeats:

$$n = \text{int}\left\{\left(\rho_{\text{mod}} - f\right)/\Delta\right\} \quad (4)$$

- Form the recovered pseudorange:

$$\rho = n\Delta + f$$

From Eqs. 3 and 4, it is clear that there are four potential sources of error in recovering pseudorange from the TANS Vector code phase: receiver position and clock bias and GPS SV position and clock bias. The combined effect of these errors cannot be larger than the 300 km length of the C/A-code; otherwise, a spurious chip can be introduced into the pseudorange.

In general, the receiver position and timing errors will be small relative to the 300 km C/A-code length, even for a receiver operating under the Standard Positioning Service (SPS). For example, the receiver positions and time biases will be accurate to about 20 m and 0.1 microseconds respectively. Contributions of GPS satellite position and timing error will be similarly small, even with the use of the broadcast ephemeris. The SPS allocates about 2 m each for these terms in the User Ephemeris Range Error (UERE)[7]. Consequently, it is a straightforward task to recover pseudorange data

from the TANS Vector code phase when the receiver is regularly computing navigation solutions. In fact, this algorithm was used to successfully recover TANS Vector pseudorange data from the RADCAL satellite, which were subsequently used to determine the RADCAL orbit with the MicroCosm© precise orbit determination filter[8]. A somewhat similar algorithm was used for the GPS flight experiments on STS-69, STS-77, and STS-80[9,10,11]. Another approach using single differences has been proposed for real-time navigation in geosynchronous orbit, except that the integer C/A-code repeats are determined "on the fly" [12].

4. AO-40 Flight Data Processing Results

GPS measurements were first returned from AO-40 in late September of 2001, and the receiver was operated for about six weeks before spacecraft power limitations necessitated shutting it down. Four GPS satellites were tracked simultaneously during the perigee pass on October 5th, as shown in Fig. 3a. This plot provides a comparison between the GPS satellites actually tracked on that day and those predicted to be visible, as shown in Fig. 3b.

The observed tracking behavior is attributed to the fact that for much of the AO-40 orbit, the receiver is above the GPS constellation, where four SVs are rarely visible simultaneously. Even around perigee, there are two factors adversely affecting tracking performance[5]. First, the blind search acquisition algorithm employed to enable high altitude tracking, coupled with the approximate 10 km/sec perigee velocity, makes it difficult for the receiver to acquire four satellites simultaneously during the perigee passes. Second, the spin rate of the AO-40 spacecraft introduces oscillations in the received signal levels, which cause intermittent signal drop outs for low elevation SVs, preventing the GPS broadcast ephemeris data from being decoded. The AO-40 TANS Vector has therefore tracked four SVs at only a few epochs, and has been unable to generate position and time bias solutions.

Without navigation solutions and broadcast ephemerides from the receiver, alternate sources of the AO-40 and GPS positions and clock biases were needed to recover the pseudorange data. AO-40 positions were generated from a NORAD Two-Line Ephemeris (TLE) obtained from the Celestrak web site[13]. The TLE was fed into an analytic propagator developed at the Air Force Research Laboratory, which uses the SGP4 algorithm for NORAD-tracked objects with periods of less than 225 minutes, and the deep space SDP4 algorithm for objects with periods greater than 225 minutes[14]. GPS SV positions and clock corrections were generated from broadcast ephemerides obtained from the International GPS Service (IGS).

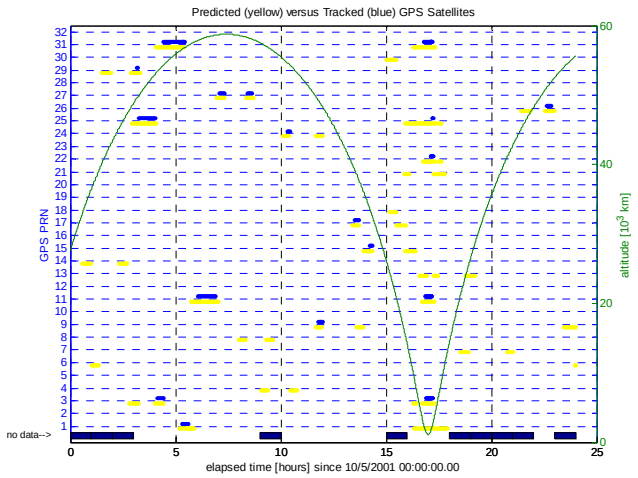

Figure 3a. AO-40 Flight GPS Tracking 10/05/01

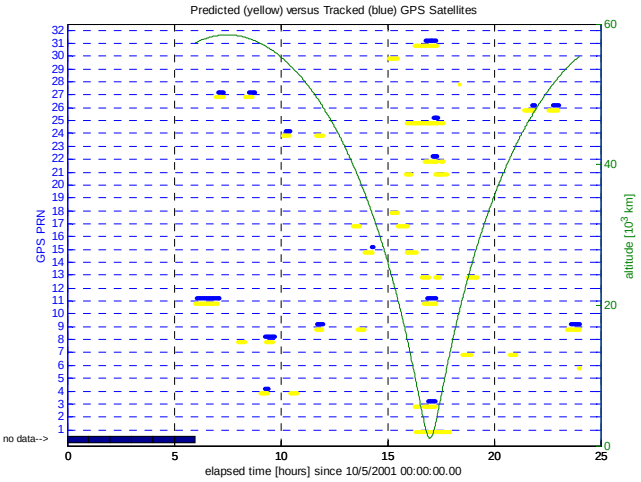

Figure 3b. AO-40 Ground Test Tracking 10/05/01

The remaining parameter required for recovering the TANS Vector pseudorange from the AO-40 code phase data was the receiver clock bias. When the TANS Vector is computing solutions, its local clock is periodically adjusted such that the bias never exceeds ±0.5 ms, and the actual value of the bias is reported as part of the point solution[6]. Unfortunately, the behavior of the bias in the absence of navigation solutions was completely unknown, so to reconstruct the pseudorange data, the time bias was assumed to be zero. The GPS data returned on October 5th were then used to reconstruct the pseudorange, using a TLE-based ephemeris for the AO-40 orbit and IGS broadcast ephemerides for the GPS satellite orbits and clocks. The pseudorange data were output with the carrier phase and Doppler data in a RINEX-2 formatted file to provide a convenient interface to a variety of orbit determination and data processing tools used at the Goddard Space Flight Center (GSFC).

4.1 Point Positioning Results

Position solutions obtained from the recovered pseudorange were compared to the SDP4-generated ephemeris used as the reference orbit. The resulting orbit differences, resolved into orbit plane components, are shown in Fig. 4. They are clearly marked by large biases in the radial and along-track directions. The cross-track differences are comparatively small, suggesting that the orbit plane is relatively well determined, but the location of the spacecraft within the plane is problematic. The three-dimensional (3D) root-sum-square (RSS) of the differences was about 110 km, and is dominated by the in-track differences.

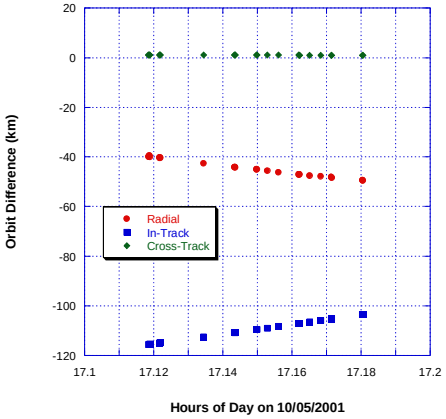

Figure 4. AO-40 Reconstructed Point Positions vs. SDP4-Generated Ephemeris

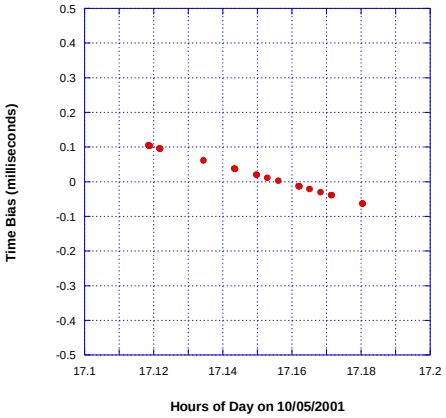

Figure 5. AO-40 Reconstructed Time Bias

The time biases obtained from the AO-40 point solutions are shown in Fig. 5. It is observed that they are on the order of 0.1 ms, and pass through zero, which was the assumed value when recovering the pseudorange. This is within the expected ±0.5 ms range the TANS Vector maintains when producing navigation solutions. In this case, however, the receiver was unable to generate navigation solutions, so the actual clock bias may have been outside this range.

Even with 4 SVs tracked and poor position dilution of precision (PDOP), it should be possible to achieve AO-40 positions that are accurate to the level of 1 km. Without better knowledge of the truth state of the AO-40 spacecraft, it is impossible to say whether the observed 100 km-level position differences shown in Fig. 4 were due to errors in the pseudorange reconstruction and resulting solutions, errors in the assumed reference trajectory itself, or both.

A self consistency analysis was performed between SDP4-generated ephemerides produced from several different TLE sets with epochs close to October 5th. The position differences were as large as 100 km at perigee, but were typically tens of kilometers elsewhere. Based on this analysis, it is reasonable to assume the reference orbit being used for AO-40 was accurate to such levels. Unfortunately, another more accurate orbit solution was unavailable to confirm this with certainty. Efforts were therefore directed towards obtaining an AO-40 orbit based on batch filtering of the recovered pseudorange.

4.2 Batch Filtering Results

To improve the reference orbit against which the point solutions are compared, the recovered pseudorange data were processed with the MicroCosm© orbit determination filter. Given that the October 5th data set spans little more than one AO-40 orbit revolution, additional data were recovered from October 6th and 7th.

The data were first pre-processed in an attempt to remove the TANS Vector clock error. To do so, the positions from SDP4-based reference orbit were processed as observations to generate an improved reference orbit based on more accurate models of the geopotential, solar radiation pressure, luni-solar effects, etc. This orbit and the pseudorange data were input to the MicroCosm© utility FixClock©, which given the host satellite and GPS ephemerides, solves for the clock error. It was also used to obtain initial conditions for subsequent orbit fits to the recovered pseudorange.

The clock-corrected TANS Vector pseudorange data were processed in a 3-day batch solution, with all six orbit elements adjusted at epoch. Another solution was then produced by fixing all of the orbit elements to their newly adjusted values, except for the mean anomaly, which was allowed to adjust after small deltas were empirically applied. This strategy was implemented based on the observation that the AO-40 orbit plane was fairly well determined, but the mean anomaly at epoch could be in error. The results from comparing these orbits to various others at perigee are shown in Table 2. Note that the first row provides the orbit difference statistics associated with Fig. 4, i.e., comparison of the point solutions to reference orbit generated with the TLE and the SDP4 propagator.

Table 2. AO-40 Batch-Filtered Orbit Comparisons [km]

	Mean			Std. Dev.		
	R	I	C	R	I	C
PP vs. TLE	-44.5	-110.0	1.0	3.4	4.1	0.0
PP vs. BF TLE	-32.9	-106.0	2.1	3.6	2.9	0.1
PP vs. BF PR #1	-28.5	-85.6	2.5	3.0	2.6	0.1
PP vs. BF PR #2	-2.8	2.5	2.8	0.2	0.5	0.1

- PP: point positions
- BF TLE: Batch filtered ephemeris from TLE/SDP4
- BF PR #1: Batch filtered pseudorange; adjust all 6 orbit elements
- BF PR #2: Batch filtered pseudorange; adjust only mean anomaly, while holding others fixed to their MC PR#1 values

From Table 2, it is seen that comparing the point positions compared to the SPD4/TLE ephemeris yields radial and in-track orbit differences on the order of 45 km and 110 km, respectively. Batch filtering this reference trajectory with MicroCosm© reduces the radial and in-track biases, but only marginally. Batch filtering the recovered pseudorange and adjusting all 6 orbit elements reduces biases to about 28 km and 85 km respectively, with effectively no change in the cross-track differences. However, the orbit produced by adjusting only the mean anomaly at epoch after fixing the other orbit elements to their previously adjusted values yielded dramatic improvement in the orbit agreements. The biases in the radial, in-track, and cross-track differences were all under 3 km, and the standard deviations were on the order of a few hundred meters. A plot of these differences is shown in Fig. 6.

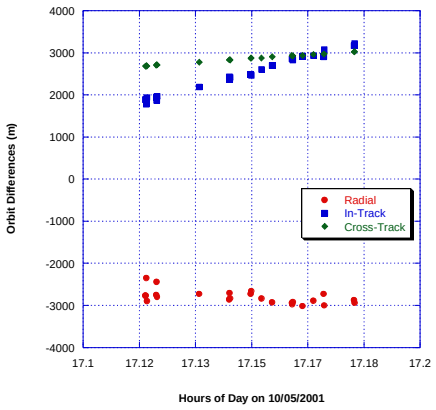

Figure 6. AO-40 Reconstructed Point Positions vs. Batch Filtered Orbit Solution

With the biases between the point positions and the batch filtered orbit significantly decreased, the orbit differences exhibit a more noise-like signature, a feature of GPS point solutions that are compared to smooth, filtered orbits. This may indicate that the point solutions are more accurate than what is suggested by the orbit comparisons.

The km-level biases that remain is likely due to residual dynamic model error in the batch filtered orbit solutions that results from mapping the pseudorange measurements backwards from their current times to the epoch time of the batch solution. The propagation times associated with such mapping can be significant for spacecraft in HEO like AO-40, which has a 19-hour period, particularly when multi-day arc lengths are used in the orbit solutions. Spans longer than 1 orbit revolution are needed, however, to resolve components such as the argument of perigee and the right ascension of the ascending node, which precess slowly over time.

It is important to point out that the level of agreement between the AO-40 point positions and the batch filtered orbit solution compares well with the estimated orbit accuracy for the POLAR spacecraft. Similar to that of AO-40, its HEO has a semi-major axis of 35,252 km and an eccentricity of 0.73. The POLAR orbit, determined from the batch filtering of ground-based range and range-rate using GTDS, is estimated to have radial, in-track, and cross-track accuracies of 1.1 km, 2.6 km, and 1.3 km[15].

4.3 TANS Vector Clock Considerations

Given that the TANS Vector was operated for several weeks prior to October 5th, there was some concern that the receiver time bias could be larger than that suggested by the point solutions obtained from the recovered pseudorange. With the AO-40 spacecraft moving at about 10 km/sec at perigee, a 0.1-second bias would look like an along-track error of 1 km, which comparable to the differences observed between the October 5th point solutions and the best batch filtered orbit. Consequently, an investigation into the behavior of the TANS Vector clock was made.

The local clock in a GPS receiver can be significantly in error when the receiver is first initialized. When the first GPS satellite is tracked, the local clock is set approximately based on time of week (TOW) derived from the hand-over-word (HOW) in the GPS navigation message. Later when the first point solution is available, the local time in the receiver is known very precisely (~100 ns). The initial setting of time from the HOW is performed as follows:

$$t_r = (TOW_{HOW} + t_d) \qquad (5)$$

where the propagation delay, t_d, is typically assumed to be constant, or approximately 0.075 seconds for a terrestrial or LEO user. At higher altitudes, the actual path delay to a GPS satellite on the opposite side of the Earth will be much longer. For the 58,000 km altitude AO-40 apogee this delay is approximately 0.3 seconds. If time is set from a satellite tracked near apogee, and

the same constant (terrestrial) path delay is assumed, it would introduce an error on the order of 230 ms.

The TANS Vector applies 1-ms adjustments to the local time in order to maintain the clock bias to less than ±0.5 ms when solutions are being performed. In between these resets, the clock is allowed to drift freely. Several tests conducted with the GPS signal simulator were used to develop a better understanding of the receiver clock behavior during long solution outages. The important findings are summarized as follows:

- When the first satellite is tracked in LEO, the TANS can set its clock very precisely. The first clock bias solution provides a measure of the error in the initial setting of the clock, plus any additional bias that has accumulated since the first satellite was tracked. In each of the tests in which the first solution occurred very soon after the first satellite was tracked, the error in the initial time obtained from the HOW was always less than ±10 ms.
- In several LEO tests in which solution outages ranged from 30 minutes to 4 hours (when less than four satellites were tracked and no solutions computed), the first reported clock bias after the outage was consistent with the predicted bias (based on the reported drift rate of the oscillator). This means that during these short outages, the TANS clock was allowed to drift freely when point solutions were not possible. After a solution outage of 4 hours, a bias of around 30 ms was accumulated.
- The clock bias after longer outages (in which point solutions were not produced) was not always consistent with expectations. This implies that the receiver continues to check its clock against the time of week derived from the HOW. If the local clock bias accumulates enough, it will be reset.

Subsequent tests revealed that in the absence of point solutions, the TANS Vector periodically adjusts its clock to keep it within tens of milliseconds of the time derived from the HOW. In a LEO, if no solutions were generated, these resets would be triggered when the clock bias grows large enough to deviate from the HOW time. Outages lasting several hours were not enough to trigger these resets. Unfortunately, in a HEO in which GPS satellites are tracked from the opposite side of the Earth, this method to calculate the time from the HOW can be in error by up to 230 ms. Apparently in the AO-40 orbit, the receiver introduces approximate 200 ms jumps in the local clock several times each orbit as it attempts to keep the local time close to the HOW time. This does, however, guarantee that that the TANS Vector clock (and the subsequent measurement time tags) should not be in error by more than about 0.25 seconds during any time GPS satellites are tracked. This assumption on the TANS Vector clock behavior in the AO-40 orbit is depicted in Fig.7.

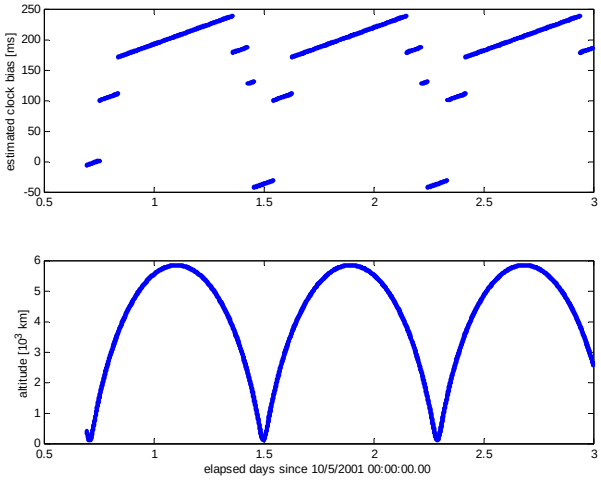

Figure 7. Assumed Behavior of the TANS Vector Clock in the AO-40 Orbit

5. Validation of the TANS Vector Pseudorange Recovery Process using Simulated Data

To gain insight into the behavior of the TANS Vector clock, and to validate the AO-40 pseudorange recovery process, a number of tests were conducted at GSFC using the Spirent (formerly GSS) STR 4760 GPS signal simulator and a duplicate of the AO-40 flight GPS receiver. The simulator modeled the motion of the receiver based on a known "truth" trajectory, and generated simulated GPS radio frequency signals that were subsequently tracked by the TANS Vector. Error sources due to GPS ephemeris and clocks and ionosphere were set to zero, so the only sources of positioning error were receiver-dependent, e.g., noise.

The first test used a trajectory based on the Landsat-7 (LS7) spacecraft. In this LEO simulation, the TANS Vector tracked four to six satellites and performed point solutions throughout, so both the receiver position and clock bias were known precisely for the pseudorange reconstruction. The second test duplicated the actual AO-40 orbital conditions from October 5th through October 8th, 2001. The predicted versus actual tracking performance for the first day is shown in Figure 3b. Note that in both the flight data (Figure 3a) and the simulated data (Figure 3b) the TANS Vector acquired four SVs at perigee on October 5th. While point solutions were not generated in real time by the flight receiver, they were produced in the ground test. Thus, unlike with the flight data, the true trajectory of the receiver is known, as is the clock behavior.

5.1 Landsat-7 Simulation Results

A test was conducted in which a TANS Vector receiver was used to collect data from a simulated LEO in which the receiver would be capable of producing

position and clock solutions regularly. The receiver trajectory was modeled based on an actual TLE for LS7 from October 5th, 2001. The LS7 orbit is circular and sun-synchronous, with a nominal altitude of 780 km. An eight hour test was conducted (spanning approximately 5 orbits), providing a data set in which both the receiver position and clock bias were precisely known throughout. From this set of observations, the following cases were derived:

Case 1 – GPS observations and time tags unmodified. This baseline case provides a reference for the TANS Vector clock behavior and the pseudorange recovery algorithm. The positions and time biases obtained from the receiver in the simulations are used to recover the pseudorange data.

Case 2 – The one ms clock corrections (applied by TANS Vector in order to maintain the bias less than ±0.5 ms) are removed from the data time tags. The result is a linear drift bias, rather than the nominal saw-tooth pattern obtained in Case 7.1.1. The initial bias is approximately 8 ms and grows to about 50 ms over the eight hour simulation run.

Case 3 – A LS7 TLE and its associated SGP4-generated ephemeris is used for the LS7 positions in the pseudorange recovery procedure. The time bias is assumed to be zero. This case is intended to duplicate the actual flight conditions, in which only an approximate ephemeris is available and the clock behavior is unknown

Pseudorange data and RINEX files were created from the LS7 observations recorded using the GPS simulator, corresponding to the cases described above. The actual clock biases inherent in each of these data sets are shown in Fig. 8. These were subsequently processed with the standard GPS navigation solution algorithm and the resulting positions were compared to the LS7 truth orbit. A 1 km edit criterion was applied to remove gross outliers. The position comparisons are summarized in Table 4.

From Table 4, it is seen that using the SGP4-generated ephemeris to recover the TANS Vector pseudorange (Case 3) yields point positions with an accuracy that is statistically similar to the point positions generated by the receiver (Case 1). A plot of the orbit accuracy obtained from the Case 3 data is shown in Fig. 9, with PDOP shown in Fig. 10. Note that the position solution outliers are highly correlated with high PDOP values. This is to be expected with a 6-channel GPS receiver like the TANS Vector.

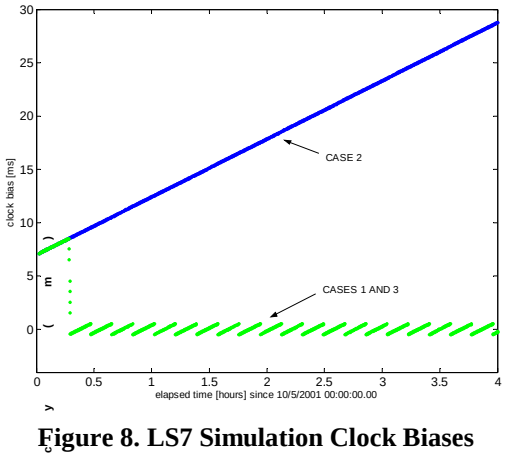

Figure 8. LS7 Simulation Clock Biases

Table 4. Navigation Solution Accuracy [m] from LS7 Simulations

	Mean			Std. Dev.		
Case	**R**	**I**	**C**	**R**	**I**	**C**
1	-1.4	-2.9	-0.6	33.6	8.8	8.6
2	-1.5	-0.7	-1.7	33.6	8.8	16.0
3	-1.4	-2.9	-0.6	33.6	8.8	8.6

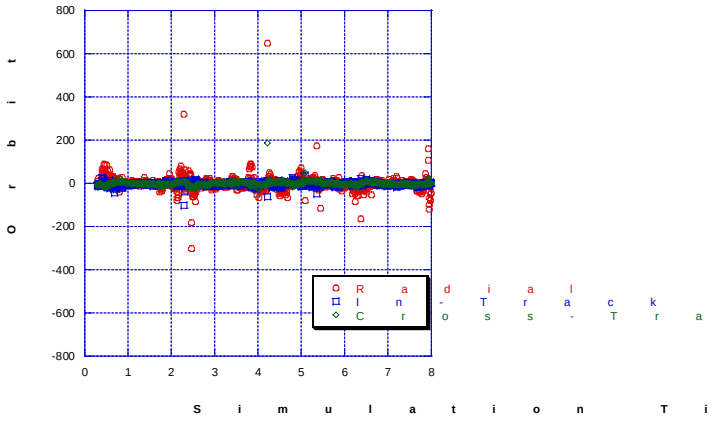

Figure 9. LS7 Case 4 Orbit Accuracy

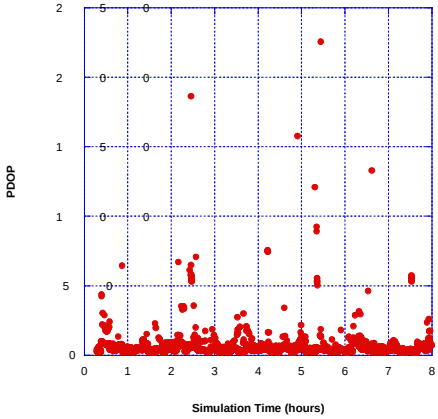

Figure 10. LS7 Case 4 PDOP

The time biases obtained in the LS7 simulations were compared to the "true" time biases, i.e., those generated by the TANS Vector in Case 1. The results are summarized in Table 5. It is seen that the true time bias is recovered with microsecond-level accuracy, even though it is assumed to be zero in the pseudorange recovery process. This shows that if the actual clock bias is unknown, but small, there is no need to estimate the bias for the pseudorange recovery process.

Table 5. Time Bias Accuracy [μsec] from LS7 Simulations

Case	Min	Max	Mean	Std. Dev.
1	-2.1	2.4	0.0	0.4
2	-2.3	2.1	0.4	0.4
3	-39.2	2.4	-0.2	2.2

5.2 AO-40 Simulation Results

Another test was conducted with the GPS simulator in an attempt to duplicate as closely as possible the actual AO-40 orbit and GPS tracking conditions. GPS-equipped spacecraft in such orbits typically view 8-12 SVs, depending on perigee latitude and perhaps 1 -2 around apogee depending on signal strength. The AO-40 simulation was run for 51 hours, which is equivalent to about 3 orbit revolutions. In this data set, the receiver truth positions are again known, and clock behavior is unknown except during a brief period around the perigee pass on October 5th. Given the knowledge gained from the LS7 simulations, the following cases were considered:

Case 1 – GPS observations and time tags were unmodified. This baseline case provides a reference for the TANS Vector clock behavior and the pseudorange recovery algorithm. Pseudorange data were recovered by using the navigation solutions output by the receiver, which occurred only around perigee.

Case 2 – This case mimics on the analysis of the 10/05/01 flight data. The TLE and SDP4 propagator were used to generate the AO-40 position data, which enabled pseudorange data to be recovered all around the orbit, and the time bias was assumed to be zero.

Case 3 – An older, and therefore less accurate, TLE was used with the SDP4 propagator to generate the AO-40 ephemeris. The epoch of this TLE is on 09/30/01, about 5 days before the Case 7.2.2 TLE epoch.

Case 4 – An even older, and therefore even less accurate, TLE was used with the SDP4 propagator to generate the AO-40 ephemeris. The epoch of this TLE is on 09/18/01, about 17 days before the Case 7.2.2 TLE epoch.

Pseudorange data and RINEX files were created from the observations recorded using the simulation of the AO-40 orbit corresponding to Cases 1-4. These were subsequently processed with the standard GPS navigation solution algorithm and the resulting positions were compared to the AO-40 truth orbit. The resulting time biases were also compared to the truth time biases, i.e., those generated by the receiver. A 1-km edit criterion was applied to remove gross outliers. The position comparisons are summarized in Table 6. A plot of the orbit accuracy obtained from the Case 4 pseudorange data is shown in Fig. 11, with PDOP shown in Fig. 12. Note again that the position solution outliers are highly correlated with high PDOP.

Table 6. Navigation Solution Accuracy [m] from AO-40 Simulations

	Mean			Std. Dev.		
Case	R	I	C	R	I	C
1	-3	-44	-5	109	61	5
2	9	-1	-1	91	47	5
3	0	7	-1	93	44	5
4	-24	16	-1	90	33	4

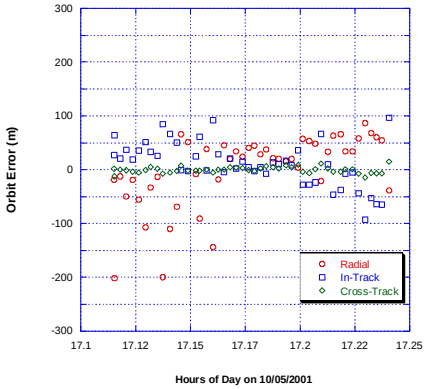

Figure 11. AO-40 Case 4 Position Accuracy

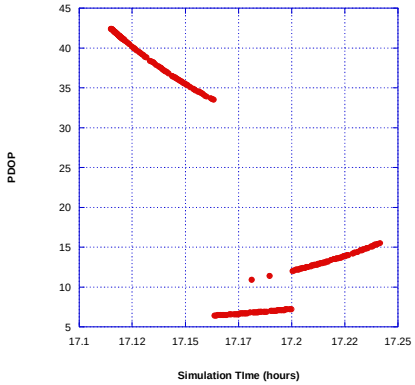

Figure 12. AO-40 Case 4 PDOP

From Table 6, it is seen that using the SDP4-propagated TLE as the reference orbit (Cases 2-4) was better than using the point solutions from the receiver

(Case 1) when recovering the TANS Vector pseudorange. Not shown, however, are the poor solutions that result from pseudorange produced by the SDP4-generated ephemeris its error is in the 100-300 km range, as in Case 4. The 1-km edit criterion that removed solutions with PDOP-related orbit error from Cases 1 and 2 also removed solutions with 100-300 km reference orbit error from Cases 3 and 4. A plot of the Case 4 orbit error is provided in Fig. 13 as an example.

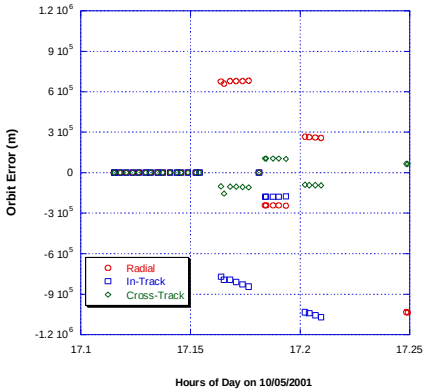

Figure 13. AO-40 Case 4 Position Accuracy (No Editing)

The discontinuities in the AO-40 orbit error shown in Fig. 13 result from spurious C/A-code repeats introduced into the recovered pseudorange as a result of the error in the reference orbit. This is shown in Table 7. The SDP4-based reference orbits were compared to an orbit generated with the high precision Goddard Trajectory Determination System (GTDS) propagator. It is observed that for Case 2, the low precision SDP4 orbit compares at the level of 1 km with respect to its GTDS counterpart, which used the same initial conditions. However, as the TLE epoch got further from October 5th, the accuracy of the SDP4-generated orbit degrades, with errors as large as 200 km observed in Case 4. When combined with the lack of knowledge of the true clock bias, such error causes the modeled pseudorange to far different from the actual pseudorange, so the incorrect number of integer C/A-code epochs are recovered.

Table 7. SDP4 vs. GTDS Ephemeris Comparisons [km] for AO-40 Simulations

	Mean			Std. Dev.		
Case	**R**	**I**	**C**	**R**	**I**	**C**
2	-0.7	1.0	0.1	0.5	0.3	0.0
3	-33.5	-72.8	0.6	4.9	6.9	0.0
4	-71.2	-177.4	-0.6	12.0	13.9	0.1

The AO-40 position solutions were then compared to their respective reference orbits, which mimics what was done with the actual AO-40 data obtained on 10/05/01. The results are shown in Table 8. It is observed that the orbit differences are comparable to the orbit error associated with the AO-40 TLE and the SDP4 propagator. This suggests that the orbit differences obtained from the 10/05/01 flight data are a result of the inaccuracy of the AO-40 reference orbit, and not the positions solutions obtained from the recovered pseudorange data.

Table 8. Navigation Solutions vs. SDP4 Ephemeris [km] for AO-40 Simulations

	Mean			Std. Dev.		
Case	**R**	**I**	**C**	**R**	**I**	**C**
2	0.4	-0.9	-0.1	0.3	0.1	0.0
3	23.8	60.5	-0.7	0.3	3.4	0.1
4	103.4	31.8	7.6	334.4	486.7	61.2

6. Conclusions

The AO-40 GPS experiment has demonstrated that GPS signals can be tracked above the constellation at altitudes as high as 58,000 km, provided that there is sufficient amplification of those weak signals. Moreover, it has been demonstrated that even a 6-channel GPS receiver using a simplified acquisition scheme can track up to 4 GPS satellites at perigee while moving as fast as 10 km/sec. It is likely that the TANS Vector would have tracked even more satellites, and possibly generated navigation solutions, were it not for the spin stabilization employed for attitude control. The spinning appears to cause signal levels to fluctuate as other antennas on the satellite block the signals. As a result, the TANS Vector is unable to lock on to the signal long enough to download the broadcast ephemeris and thus generate point solutions. This resulted in having to use the TLE as an external source of ephemeris data when trying to recover the pseudorange.

The AO-40 reference orbit generated from the TLE and the SDP4 propagator appears to be in error by about 100 km, the majority of which is in the direction of spacecraft motion. This would seem large relative to what is typical for a LEO satellite, but TLEs are generally computed from sparse, low precision tracking data. With limited number of tracking passes at perigee, producing mostly azimuth and elevation observations and a comparatively smaller amount of radar range data, this is to be expected for a spacecraft in HEO. Nonetheless, such accuracy is well within the 300 km tolerance of the C/A-code repeat when recovering pseudorange data from the TANS Vector code phase. In fact, simulations show that there is no distinguishable difference between the use of actual receiver point solutions and an SGP4/SDP4-based ephemeris when it comes to recovering pseudorange. Moreover, by assuming the time bias to be zero in the pseudorange recovery process, simulations show that

the actual time bias can be well determined from the resulting pseudorange.

However, the simulations also show that assessing the accuracy of navigation solutions obtained from the TANS Vector requires an accurate reference or truth ephemeris. An SDP4-based ephemeris accurate to 100 km was sufficient to recover the AO-40 pseudorange produced in the simulations, but when the resulting point solutions were compared to this ephemeris, a similar level of orbit difference was obtained. In contrast, when compared to the truth, the same point solutions yielded sub-100 m accuracy, much of which is due to the high PDOP observed with a 6-channel receiver in the AO-40 orbit.

This suggests that for the 10/05/01 flight data, the 14 point solutions produced were probably accurate at a similar level, but this was masked by the poor quality of the SDP4-based ephemeris, which differed from the point solutions at the level of 100 km. Comparing the point solutions to an orbit generated by batch filtering the recovered pseudorange reduced the orbit differences to about 3 km RMS. This agrees well with the estimated orbit accuracy for the POLAR spacecraft, which occupies a HEO that is very similar to that of AO-40. Moreover, the AO-40 simulations show that the standard deviations of the orbit differences are within the expected range of GPS point solutions when PDOP is taken into account. To further improve the batch filtered orbit solutions, more experience in GPS-based precise orbit determination for HEOs is needed. Future research will therefore focus on the processing of newly acquired AO-40 flight data with the GEONS Extended Kalman Filter developed at NASA GSFC, as well as with MicroCosm©.

7. Acknowledgements

The authors would like to acknowledge the contributions of Anne Long and David Kelbel of the Computer Sciences Corporation, of Tom Martin of Van Martin Systems, Inc., Rich Burns and Ed Davis of NASA GSFC, and Larry Jackson of Orbital Sciences Corp, and the AMSAT AO-40 Team, especially Jim White and Mike Kingery.

8. References

1. ESTEC, TEAMSAT Results, April 1998, http://www.estec.esa.nl/teamsat/.
2. Balbach, O., et al., "Tracking GPS Above GPS Satellite Altitude: First Results of the GPS Experiment on the HEO Mission Equator-S," *IEEE PLANS*, 1998, pp. 243-249.
3. Powell, T., et al., "GPS Signals in a Geosynchronous Transfer Orbit: Falcon Gold Data Processing," ION Nation Technical Meeting, January, 1999, pp. 575-585.
4. Kronman, J.D., "Experience Using GPS for Orbit Determination of a Geosynchronous Satellite," *Proceedings of the Institute of Navigation GPS 2000 Conference*, Salt Lake City, UT, Sep. 2000.
5. Moreau, M., et al., "Preliminary Results of the GPS Flight Experiment on the High Earth Orbit AMSAT-OSCAR 40 Spacecraft," 25th Annual Guidance Navigation and Control Conference, Breckenridge, CO, February, 2002.
6. Trimble Navigation Limited, *TANS VECTOR Specification and User's Manual, May, 1995.*
7. Parkinson, B., et al., (eds.), Global Positioning System: Theory and Applications, AIAA, Vol. 1.
8. Davis, G., et al., *A Low Cost, High Accuracy Automated GPS-Based Orbit Determination System for Low Earth Satellites, ION GPS-97, Nashville, TN, September, 1997.*
9. Park, Y., et al., *Flight Test Results from Realtime Relative GPS Flight Experiment on STS-69*, SPACE FLIGHT MECHANICS 1996, Vol. 93 in Advances in the Astronautical Sciences, Univelt, San Diego, pp. 1277-1295.
10. Schiesser, E., et al., *Results of STS-80 Relative GPS Navigation Flight Experiment*, SPACE FLIGHT MECHANICS 1998, Vol. 99 in Advances in the Astronautical Sciences, Univelt, San Diego, pp. 1317-1334.
11. Lisano, M., and Carpenter, R., *High-Accuracy Space Shuttle Reference Trajectories for the STS-77 GPS Attitude and Navigation Experiment (GANE)*, SPACE FLIGHT MECHANICS 1997, Vol. 95 in Advances in the Astronautical Sciences, Univelt, San Diego, pp. 195-206.
12. Fichter, W., et al., "Geostationary GPS Based Navigation Using Pseudorange Fractional Part Measurements," *Space Technology*, Vol. 21, No.1-2, pp.33-40, 2001.
13. Kelso, T.S., http://celestrak.com/
14. Hoots, F., and Roerich, R., Spacetrak Report No. 3, Project Spacetrack Reports, Office of Astrodynamics, Aerospace Defense Center, ADC/DO6, Peterson AFB, CO 80914
15. Airapetian, V. et al., Space Orbit Determination Accuracy from Mission Experience, Computer Sciences Corp. Report CSC-5506-44, February, 2002.